PAPR Reduction Scheme for Localized SC-FDMA Based on Deep Learning

Hao Lu[1], Yu Zhou[2], Yue Liu[1], Rui Li[1(✉)], and Ning Cao[1]

[1] Hohai University, Nanjing 210098, China
luhao@hhu.edu.cn
[2] Marketing Service Center, State Grid Jiangsu Electric Power Co. Ltd., Nanjing, China

Abstract. Large peak-to-average power ratio (PAPR) hinders the development of the localized single carrier frequency division multiple access (SC-LFDMA). In this paper, autoencoder (AE) is introduced in SC-LFDMA to reduce PAPR, known as AE-SC-LFDMA. In AE-SC-LFDMA, the Encoder and Decoder of AE are used to encode and decode the modulated symbols of conventional SC-LFDMA based on deep neural network (DNN). This process aims to make AE-SC-LFDMA achieve lower PAPR as well as be more robust to the nonlinear distortion (NLD) of high power amplifier (HPA). Simulation results show that the proposed scheme outperforms conventional schemes both in bit error rate (BER) and PAPR.

Keywords: SC-LFDMA · AE · DNN · HPA

1 Introduction

Single carrier frequency division multiple access (SC-FDMA) has been adopted in the long term evolution (LTE) uplink [1]. It can be described as a version of orthogonal frequency division multiplexing (OFDMA) in which pre-coding and inverse pre-coding stages are added at the transmitter and receiver ends respectively. SC-FDMA has similar throughput and complexity as OFDMA [2]. With lower peak-to-average power ratio (PAPR), SC-FDMA has been seen as a good replacement of OFDMA in some power-efficient scenarioes.

Nevertheless, to acquire long-range detection capabilities and improve power efficiency, the high power amplifier (HPA) in the radar transmitter always operates in saturation. PAPR of the localized SC-FDMA (SC-LFDMA) is not negligible under the nonlinear (NL) HPA. It requires a large input back off (IBO) of the transmit hard power amplifier (HPA) from its output saturation point, which leads to very low power efficiency [3].

Some research has focused on the PAPR reduction of the SC-LFDMA. Selective mapping (SLM) [4] is a notable technique for PAPR reduction. However, the

Q. Guo et al. (Eds.): WiSATS 2021, LNICST 410, pp. 697–708, 2022.
https://doi.org/10.1007/978-3-030-93398-2_60

receiver needs to know the phase factor correctly. Otherwise, the BER performance is greatly degraded. Secondly, pulse shaping method is also proposed. [5] analytically derives the time and frequency domain parametric linear pulse for PAPR reduction. [6] considers an envelope-constrained filter design to optimize the impulse response of a hybrid filter in terms of PAPR reduction. Although this technique is widely used to reduce PAPR, the spectral efficiency and computation complexity are still needed to be improved.

Recently, deep learning (DL), an important branch of machine learning (ML) has shown great potentials in optimizing wireless communication system. As a purely data-driven method, we can learn the properties and the parameters of a DL model directly from the data, without handcraft or ad-hoc designs [7,8]. Autoencoder (AE), a special case of DL, consists of auto-encoder and auto-decoder. Both of them are represented by neural networks (NNs) and trained in an end-to-end manner. Due to the similarity between auto-encoder and transmitter as well as auto-decoder and receiver, AE has been used in some publications to solve communication problems [9]. A novel PAPR reducing network (PRNet) based on AE is proposed in [10]. Convolutional autoencoder (CAE) for PAPR reduction under NL HPA is introduced in [11]. NNs trained on the active constellation extension (ACE) signals is used to reduce the PAPR of OFDM signals in [12]. [13] extends the end-to-end learning to OFDM with cyclic prefix (CP) and compares with conventional OFDM over frequency-selective fading channels. [14] handles the joint transmitter and noncoherent receiver optimization for multiuser single-input multiple-output communications through unsupervised deep learning. Tone reservation network is proposed in [15] to improve the performance of the tone reservation technique. The successful applications indicate that the AE is capable of optimizing the communication system.

To the best of our knowledge, there is no previous work solving the PAPR problem of SC-LFDMA through DL. In this paper, we introduce DL not only to reduce PAPR of SC-LFDMA but also to make it more robust to the nonlinear distortion (NLD) from HPA. The main contribution of this paper is listed as follows,

- We propose a novel PAPR reduction system for SC-LFDMA named AE-SC-LFDMA. In this system, coding and decoding of the modulated symbols in each subcarrier are optimized jointly based on DNN.
- The performance of the proposed system is evaluated using computer simulations. We find that AE-SC-LFDMA has lower PAPR than SC-LFDMA and other PAPR reduction schemes. Moreover, AE-SC-LFDMA shows more robust to the nonlinear effects.

This paper is organized as follows. System model is introduced in the Sect. 2. Then, proposed scheme is given in Sect. 3. Performance is evaluated in Sect. 4. Finally, Sect. 5 concludes this paper.

2 System Model

2.1 System Model

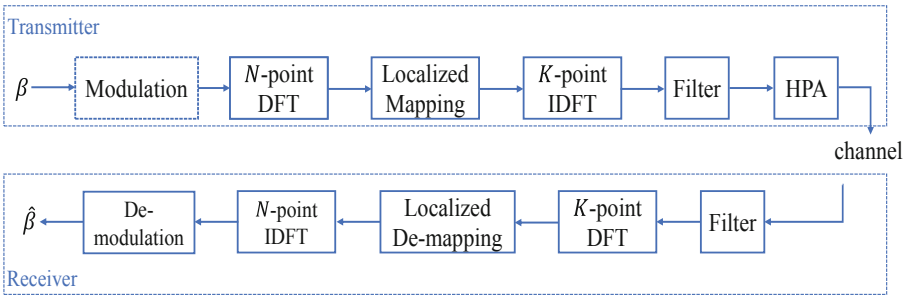

Fig. 1. System Model.

Transmitter. Considering a single user SC-LFDMA in one time block, the system model is shown in Fig. 1. Firstly, the modulated signal is given,

$$s(t, \beta) = \exp(j\phi(t; \beta)), \tag{1}$$

where β is the binary information and $\phi(t; \beta)$ is the signal phase.

Then, $\boldsymbol{s} = [s_0, s_1, \cdots, s_{Q-1}]$, sampled $s(t, \beta)$, is first linearly precoded by an Q by Q DFT precoding matrix. The resulting frequency-domain data vector $\boldsymbol{S} = [S_0, S_1, \cdots, S_{Q-1}]^T$ is,

$$S_i = \sum_{q=0}^{Q-1} s_n e^{-j\frac{2\pi iq}{Q}}, \quad 0 \leq i \leq Q-1. \tag{2}$$

There are total K subcarriers in SC-LFDMA and K is an integer multiple of Q. The frequency domain data $\boldsymbol{S}$ are mapped across the frequency band by localized method [1]. For LFDMA, chunks of adjacent subcarriers are allocated to each user,

$$\boldsymbol{S}^{'} = [\overbrace{0, 0, \cdots, 0, S_1, S_2, \cdots, S_Q, 0, 0, \cdots, 0}^{K}], \tag{3}$$

Then, the frequency domain elements $\boldsymbol{S}^{'}$ are processed with the K-point IDFT and converted to analog domain. Assuming there are N_s symbols and symbol duration is T_s, the formed SC-LFDMA signal is,

$$\begin{aligned} x(t) \ &= e^{j2\pi f_c t} \sum_{\mu=0}^{N_s-1} \sum_{k=0}^{K-1} S^{'}_{\mu,k} e^{j2\pi f_k t} \\ &\cdot g(t - \mu T_s), \end{aligned} \tag{4}$$

where $S^{'}_{\mu,k}$ is the symbol in the k^{th} subcarrier of μ^{th} symbol; f_c is the carrier frequency; N_s is the number of SC-FDMA symbols contained in each pulse; $f_k = k\Delta f$, $\Delta f = \frac{1}{T_s}$ is the frequency interval between subcarrier; $g(t)$ is root raised cosine filter (RRC) pulse shaping filter.

HPA. $x(t)$ is fed to an HPA to produce an amplified time domain signal $x^{'}(t)$,

$$x^{'}(t) = x(t) + \Phi_{NL}(t), \tag{5}$$

where $\Phi_{NL}(t)$ denotes the NL term caused from HPA and distributed following the complex circular Gaussian random variable [16].

Based on (4), $x^{'}(t)$ can be expressed as,

$$\begin{aligned} x^{'}(t) &= e^{j2\pi f_c t} \sum_{\mu=0}^{N_s-1} \sum_{k=0}^{K-1} S^{T}_{\mu,k} e^{j2\pi f_k t} \cdot g(t - \mu T_s) \\ &= e^{j2\pi f_c t} \sum_{\mu=0}^{N_s-1} \sum_{k=0}^{K-1} (S^{'}_{\mu,k} + S^{NL}_{\mu,k}) e^{j2\pi f_k t} \\ &\cdot g(t - \mu T_s), \end{aligned} \tag{6}$$

where $S^{T}_{\mu,k}$ is the final transmitted symbol in the k^{th} subcarrier of μ^{th} symbol and $S^{NL}_{\mu,k}$ is the corrupted term due to the band-limited RRC filter and HPA.

Receiver. Considering communication link, Vehicle B receives the digital domain RCI signal,

$$r_n = x^{'}_n + w_n, \tag{7}$$

where w_n is additive white Gaussian noise (AWGN) with zero mean and one-sided PSD. We can see that the nonlinear part $\Phi_{NL}(t)$ (5) decreases the signal to interference plus noise ratio (SINR). Signal processing in the communication receiver is shown in Fig. 1. The received signal r_n is first filtered by RRC and is transformed into the frequency domain via DFT, $r_n \xrightarrow{\text{DFT}} R_{\mu,k}$. Next, collecting these coefficients of $R_{\mu,k}$ that correspond to each user by inverse localized mapping. We obtain the recovered modulated symbol $R_{\mu,k} \xrightarrow{\text{IDFT}} \tilde{\boldsymbol{s}}$, which includes NLD and Gaussian noise. Noted that for simplicity, we denote the steps, DFT, mapping, IDFT and RRC as SC-LFDMA MOD and the inverse process as SC-LFDMA DEMOD.

2.2 Design Insights

Recovery of transmitted communication information is paramount for communication system. From (6) and (7), band-limited filter, HPA and AWGN affect the communication quality. Signal's PAPR and robustness determine the degree of these effects on them. Therefor, we can improve SC-LFDMA system in two

ways. First, the transmitted symbol are modulated and encoded to have lower PAPR and be robust to these effects. Second, the receiver is able to identify the correct information from the corrupted signal. Hence, we not only need to search the efficient modulation and code of the $S'_{\mu,k}$ but also require an efficient receiver. Traditional model-based methods tend to optimize the transmitter and receiver separately and rarely consider the joint transceiver design. To achieve an efficient SC-LFDMA system, we introduce AE to optimize the transmitter and receiver jointly.

3 Proposed Scheme

In this section, we first briefly discuss the AE general concept. Then, we provide our proposed scheme.

3.1 Introduction of Autoencoder

As one specific type of feedforward NNs, AE consists of Encoder and Decoder. We denote x as the input, $f(x)$ as the Encoder, and $g(x)$ as the Decoder, respectively. The final output of AE is $g(f(x))$. To achieve one or more specific objects, the loss function is set as $L(x, g(f(x)))$. With the goal of minimizing $L(x, g(f(x)))$, AE can be trained through some optimization methods such as adaptive moment estimation (Adam), Stochastic Gradient Descent (SGD) and so on. For example, in [8], to improve the block error rate (BLER) performance, a conventional communication system is represented as an AE. AE is trained to recover the input at the output under various channel conditions. The loss function is set as $L = -\log(b_s)$, where b_s is the s^{th} element of the message probability vector $\boldsymbol{b}$. To minimize the loss function, SGD is used as the optimization method to update the parameters of AE. Finally, the estimation of original input can be obtained from the largest element in $\boldsymbol{b}$.

3.2 Overall Structure of AE-SC-LFDMA

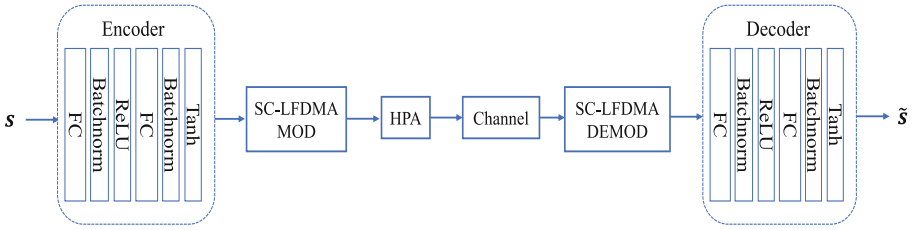

Fig. 2. Proposed AE-SC-LFDMA scheme.

The overall structure of the AE-SC-LFDMA is shown in Fig. 2. Similar to a conventional communication system, the AE-SC-LFDMA system contains three

modules, namely, the integrated transmitter/radar receiver, the communication receiver, and the channel. The integrated transmitter takes the modulated symbol $\boldsymbol{s}$ to generate transmitted signal. Noted that modulated symbol $\boldsymbol{s}$ is complex values vector, we assume each element in this vector is $s_q = a_q + b_q i$. Since pytorch cannot operate with complex values, we should convert the input vector $\boldsymbol{s}$ to the real value vector $\{a_0, b_0, a_1, b_1, \cdots, a_Q, b_Q\}$. The Encoder outputs $f(\boldsymbol{s})$ are fed through the SC-FDMA MOD block. Then, the transmitted RCI signal can be expressed as

$$x(t) = \text{MOD}(f(\boldsymbol{s})). \tag{8}$$

The received signal passes through SC-LFDMA DEMOD block. Similar to the Encoder, the symbol should be divided into real and imaginary parts. The obtained vector is fed into Decoder. Finally, the recovered symbol is,

$$\tilde{\boldsymbol{s}} = g(\text{DEMOD}(H(x(t)))), \tag{9}$$

where $H(\cdot)$ means the channel effect.

The used AE block is shown in Fig. 2. The Encoder and Decoder contain the sub-blocks with the same structure. Each sub-block contains fully connected (FC) layers, batch normalization (BN), and activation function. In the FC, $\boldsymbol{x}_{FC}$ is the input of the m^{th} layer, and the FC output $\boldsymbol{y}_{FC}$ can be expressed as $\boldsymbol{y}_{FC} = \boldsymbol{w}_m \boldsymbol{x}_{FC} + \boldsymbol{b}_m$, where $\boldsymbol{w}_m$ and $\boldsymbol{b}_m$ are weights and bias of the m^{th} layer. The output of the FC enters the Batchnorm unit and is used to normalize the input of the activation function. The mathematical representation of Batchnorm is $\text{BN}(\boldsymbol{y}_{FC}) = \gamma \frac{\boldsymbol{y}_{FC} - \mathbb{E}\{\boldsymbol{y}_{FC}\}}{\sqrt{Var\{\boldsymbol{y}_{FC}\} + v}} + \beta$, where γ and β denote the scaling and shift factors, respectively. $\mathbb{E}\{\boldsymbol{y}_{FC}\}$ and $Var\{\boldsymbol{y}_{FC}\}$ denote the mean and variance of $\boldsymbol{y}_{FC}$, respectively. In addition, $v = 0.001$ prevents division by zero. γ and β can be obtained through training and learning. The normalized value then enters the activation function $\phi(\cdot)$. In this solution, ReLU and Tanh serve as the activation function. The output of the ReLU on the m^{th} layer is $\max(\text{BN}(\boldsymbol{y}_{FC}), 0)$, while the output of the Tanh on the m^{th} layer is $\frac{e^{\boldsymbol{y}_{FC}} - e^{-\boldsymbol{y}_{FC}}}{e^{\boldsymbol{y}_{FC}} + e^{-\boldsymbol{y}_{FC}}}$. The used Encoder is composed of $L_f = 2$ sub-blocks. The final output can be expressed as $f(\boldsymbol{r}) = \phi_{L_f}(\text{BN}(\boldsymbol{w}_{L_f}^f \phi_{L_f - 1}(\cdots \phi_1(\text{BN}(\boldsymbol{w}_1^f \boldsymbol{r} + \boldsymbol{b}_1^f)) \cdots)))$, where $\boldsymbol{w}_{L_f}^f$ and $\boldsymbol{b}_{lf}^f$ are the weights and biases for the l_f-th FC of the Encoder. Similar to the Encoder, the Decoder can be expressed as $g(\boldsymbol{r}) = \phi_{L_f}(\text{BN}(\boldsymbol{w}_{L_f}^f \phi_{L_f - 1}(\cdots \phi_1(\text{BN}(\boldsymbol{w}_1^f \boldsymbol{r} + \boldsymbol{b}_1^f)) \cdots)))$, where $\boldsymbol{w}_{L_f}^f$ and $\boldsymbol{b}_{lf}^f$ are the weights and biases for the l_f-th FC of the Decoder.

3.3 Training of Network

To optimize both the transmitter and receiver performance under the NLD effect, we jointly train the Encoder and Decoder to adjust the parameters $\theta = \{\theta_f, \theta_g\}$, where θ_f and θ_g denotes the parameters in the Encoder block and Decoder block, respectively. In the following, two objective functions required for network training are provided.

Firstly, to make signal be robust to the NLD, the first objective function is set to minimize the distance between recovered symbols and original symbols $\mathcal{L}_1(\boldsymbol{s}, \tilde{\boldsymbol{s}})$,

$$\mathcal{L}_1(\boldsymbol{s}, \tilde{\boldsymbol{s}}) = \|\boldsymbol{s} - \tilde{\boldsymbol{s}}\|_2 , \tag{10}$$

where $\boldsymbol{s}$ denotes the original symbols and $\tilde{\boldsymbol{s}}$ is the recovered symbols. As the first objective function $\mathcal{L}_1(\boldsymbol{s}, \tilde{\boldsymbol{s}})$ is minimized, communication receiver are more likely to obtain the correct communication information.

Secondly, the transmitted signal is expected to have lower PAPR. We propose to minimize PAPR as the goal. Then, the second objective function is to minimize $\mathcal{L}_2(\boldsymbol{s})$,

$$\mathcal{L}_2(\boldsymbol{s}) = \text{PAPR}\{x[n]\} = \text{PAPR}\{\text{MOD}(f(\boldsymbol{s}))\} \tag{11}$$

The PAPR of the transmitted signal vector $\boldsymbol{x} = [x_0, x_1, \cdots, x_{N-1}]^T$ is defined as,

$$\text{PAPR}\{\boldsymbol{x}\} = \frac{\max\limits_{0 \le n \le N-1} |x_n|^2}{\mathbb{E}\{|x_n|^2\}},$$

where $\mathbb{E}\{|x_n|^2\}$ is the average power of $x[n]$ over $0 \le n \le N-1$.

The objective funtion $\mathcal{L}_1(\boldsymbol{s}, \tilde{\boldsymbol{s}})$ is not only used to train the demodulator to reconstruct the transmitted symbol correctly but also train the transmitted symbol more robust to the bandlimited filter, NLD and AWGN. The objective funtion $\mathcal{L}_2(\boldsymbol{s})$ constrains the PAPR of the transmitted signal. To achieve both the recovery of transmitted symbol and the reduction of PAPR, the Encoder and Decoder modules need to be jointly trained. Hence, the joint loss function $\mathcal{L}(\boldsymbol{s}, \tilde{\boldsymbol{s}})$ is defined as,

$$\mathcal{L}(\boldsymbol{s}, \tilde{\boldsymbol{s}}) = \mathcal{L}_1(\boldsymbol{s}, \tilde{\boldsymbol{s}}) + \omega * \mathcal{L}_2(\boldsymbol{s}) \tag{12}$$

where ω represents weighting factor of the objective function $\mathcal{L}_2(\boldsymbol{s})$.

The training progress is listed as follows:

- Data preparation: We generate the binary information randomly and modulate them by quadrature phase shift keying (QPSK). The Data set is divided into three parts. 70% of the data is used for training; 20% is used for validation; 10% is used for testing.
- Model and loss function: AE-SC-LFDMA is used for training. We set the loss function as $\mathcal{L}(\boldsymbol{s}, \tilde{\boldsymbol{s}})$ (12) and deploy Adam to minimize $\mathcal{L}(\boldsymbol{s}, \tilde{\boldsymbol{s}})$.
- Training: The training data is trained iteratively. In each iteration, Adam updates the parameters of AE-SC-LFDMA to gradually approach minimum of $\mathcal{L}(\boldsymbol{s}, \tilde{\boldsymbol{s}})$. The model is evaluated on validation set after every five iterations. Finally, we can obtain an AE-SC-LFDMA with optimal parameters after training.
- Testing: Ultimately, the communication and radar performance are presented through deploying the final AE-SC-LFDMA model on the testing data set.

4 Simulation Results

In this section, the performance of our proposed AE-RCI system is compared to a conventional SC-FDMA scheme by considering important attributes such as complementary cumulative distribution function (CCDF) of the PAPR and BER. We compare the proposed scheme with the common traditional scheme, SLM [4]. Besides, the proposed scheme is also compared with the convolutional neural network (CNN) shown in [11].

4.1 Parameter Setting

We consider an SC-LFDMA scheme with parameter setting listed in Table 1. QPSK is selected as modulation and AWGN channel is assumed. Parameters used for the AE setup is provided in Table 2. Both Encoder and Decoder are made of three layers and 128 neurons for hidden layer. For training the autoencoder, we use the batch size of 1000. Adam [17] optimizer and learning rate of 0.05 are used. Moreover, the SNR for training is set to be 10 dB. The training SNR is determined by training AE with 2 dB SNR increment per step starting from 0 dB to 20 dB until the SNR with the balanced performance with the BER and PAPR.

In this paper, HPA uses the TWTA model [18]. The amplified output, i.e., the final transmitted signal is,

$$x^{'}(t) = A(\rho(t))e^{j(\phi(t)+\Phi(\rho(t)))} \tag{13}$$

where $\rho(t)$ and $\phi(t)$ represent the envelope and phase of $x(t)$, respectively. And $A(\cdot)$ and $\Phi(\cdot)$ represent amplitude to amplitude modulation (AM/AM) and amplitude to phase modulation (AM/PM) conversions, respectively. The expressions for $A(\cdot)$ and $\Phi(\cdot)$ are given,

$$A(r) = \frac{\alpha_a r}{1+\beta_a r^2}, \qquad \Phi(r) = \frac{\alpha_\phi r^2}{1+\beta_\phi r^2}.$$

A plausible choice of the above parameters is $\alpha_a = 2.1587$, $\beta_a = 1.1517$, $\alpha_\phi = 4.0033$, $\beta_\phi = 9.1040$ [19].

Input back off (IBO) is an important parameter which describes the amplifier operating point by relating the saturation power of the HPA to the average power of the input signal. It is defined as

$$\text{IBO} = \frac{P_{in}^{sat}}{P_{in}}, \tag{14}$$

where P_{in}^{sat} is the input saturation power and $P_{in} = \mathbb{E}[|x[n]|^2$.

4.2 PAPR Comparison

The PAPR measure is commonly used as an indicator for the required amount of IBO for HPA operation. Higher PAPR means that larger IBO is needed in

Table 1. Parameter setting of RCI system

Parameter	Symbol	Value
Carrier frequency	f_c	24 GHz
Frequency interval	Δf	400 kHz
Symbols of each user	Q	40
Symbol number	N_s	5
Subcarrier number	K	80

Table 2. Parameters used for the AE setup

Encoder module		Decoder module	
Parameter	Value	Parameter	Value
Size of input layers	16	Size of input layers	16
Size of hidden layers	128	Size of hidden layers	128
Size of output layers	16	Size of output layers	16
Hidden layer activation	'ReLU'	Hidden layer activation	'ReLU'
Optimizer algorithm		Adam	
Learning rate		0.05	
Training SNR		10 dB	
Batch size		1000	
Weighting		$\omega = 2$	

HPA. In other words, HPA can not operate in the saturation (IBO = 0dB). This can lead to the power loss of the system. Hence, low PAPR is conducive to the improvement of system power efficiency. The numerically calculated CCDF of the PAPR of AE-SC-LFDMA, original SC-LFDMA, SC-LFDMA with SLM and CAE-SC-LFDMA are given in Fig. 3. We can see that, compared with SC-LFDMA, the corresponding gain is about 3 dB for CCDF = 10^{-3} and 2–3 dB for high CCDF percentiles. For SC-LFDMA with SLM, the gain is about 1dB for CCDF = 10^{-3}. Although SC-LFDMA with SLM outperforms in the high CCDF percentiles. The side information needed in the SLM detection lowers the system efficiency. Moreover, for CAE-SC-FDMA, AE-SC-LFDMA outperforms about 1–2 dB in the overall CCDF. Thus, the NL distortion is expected to be smaller and the power efficiency can be improved in the proposed AE-SC-LFDMA scheme.

4.3 BER Comparison

BER performance comparison of these schemes in the AWGN channel under IBO = 0dB is shown in Fig. 4.

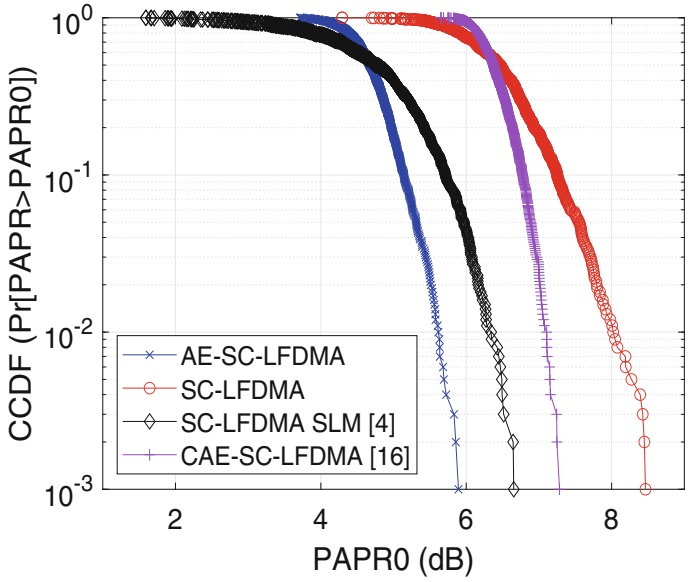

Fig. 3. PAPR performance comparison.

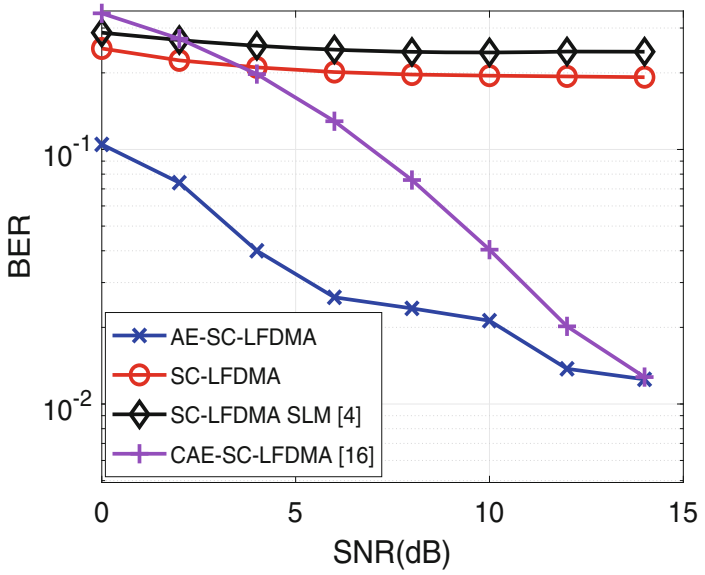

Fig. 4. BER performance comparison (IBO = 0 dB).

The BER performance of the AE-SC-LFDMA is obviously better than that of other SC-LFDMA schemes in the entire SNR range. Compared with original SC-LFDMA and SC-LFDMA with SLM, proposed AE-SC-LFDMA outper-

forms significantly in the entire range. Besides, AE-SC-LFDM achieves about 5dB performance over CAE-SC-LFDMA in the low SNR range. In a word, the proposed AE-SC-FDMA can achieve satisfied BER performance even under the IBO = 0dB. This shows that AE-SC-FDMA is more robust to the NLD.

5 Conclusion

This paper proposes a novel autoencoder (AE)-based PAPR reduction scheme for localized SC-FDMA, namely AE-SC-LFDMA. Through optimizing transceiver jointly based on deep neural network (DNN), AE-SC-LFDMA is capable of reduing PAPR while improving robustness to the nonlinear effects of high power amplifier. Simulation shows that the proposed AE-SC-LFDM can achieve lower PAPR and BER than conventional SC-LFDMA. Futher work focusing on usage of sparse autoencoder is needed.

Acknowledgements. This work was supported by Research on Performance Evaluation and Optimization Technology of Local IOT for Client-side Metering Equipment under grant No. 5700-202118203A-0-0-00.

References

1. Myung, H.G., Goodman, D.J.: Single Carrier FDMA: A New Air Interface for Long Term Evolution, vol. 8. Wiley, Hoboken (2008)
2. Chen, G., Song, S., Letaief, K.B.: A low-complexity precoding scheme for PAPR reduction in SC-FDMA systems. In: 2011 IEEE Wireless Communications and Networking Conference, pp. 1358–1362. IEEE (2011)
3. Ji, J., Ren, G., Zhang, H.: PAPR reduction of SC-FDMA signals via probabilistic pulse shaping. IEEE Trans. Veh. Technol. **64**(9), 3999–4008 (2014)
4. Mohammad, A., Zekry, A., Newagy, F.: A time domain SLM for PAPR reduction in SC-FDMA systems. In: 2012 IEEE Global High Tech Congress on Electronics, pp. 143–147. IEEE (2012)
5. Meza, C.A., Lee, K., Lee, K.: PAPR reduction in single carrier FDMA uplink system using parametric linear pulses. In: ICTC 2011, pp. 424–429. IEEE (2011)
6. Kamal, S., Meza, C.A.A., Tran, N.H., Lee, K.: Low-PAPR hybrid filter for SC-FDMA. IEEE Commun. Lett. **21**(4), 905–908 (2016)
7. Ye, H., Liang, L., Li, G.Y., Juang, B.: Deep learning-based end-to-end wireless communication systems with conditional GANs as unknown channels. IEEE Trans. Wirel. Commun. **19**(5), 3133–3143 (2020)
8. Dörner, S., Cammerer, S., Hoydis, J., Ten Brink, S.: Deep learning based communication over the air. IEEE J. Sel. Top. Sig. Process. **12**(1), 132–143 (2017)
9. O'shea, T., Hoydis, J.: An introduction to deep learning for the physical layer. IEEE Trans. Cogn. Commun. Networking **3**(4), 563–575 (2017)
10. Kim, M., Lee, W., Cho, D.H.: A novel PAPR reduction scheme for OFDM system based on deep learning. IEEE Commun. Lett. **22**(3), 510–513 (2017)
11. Huleihel, Y., Ben-Dror, E., Permuter, H.H.: Low PAPR waveform design for OFDM system based on convolutional auto-encoder. arXiv preprint arXiv:2011.06349 (2020)

12. Sohn, I.: A low complexity PAPR reduction scheme for OFDM systems via neural networks. IEEE Commun. Lett. **18**(2), 225–228 (2014)
13. Felix, A., Cammerer, S., Dörner, S., Hoydis, J., Ten Brink, S.: OFDM-autoencoder for end-to-end learning of communications systems. In: 2018 IEEE 19th International Workshop on Signal Processing Advances in Wireless Communications (SPAWC), pp. 1–5. IEEE (2018)
14. Xue, S., Ma, Y., Yi, N., Tafazolli, R.: Unsupervised deep learning for MU-SIMO joint transmitter and noncoherent receiver design. IEEE Wirel. Commun. Lett. **8**(1), 177–180 (2018)
15. Wang, B., Si, Q., Jin, M.: A novel tone reservation scheme based on deep learning for PAPR reduction in OFDM systems. IEEE Commun. Lett. **24**(6), 1271–1274 (2020)
16. Balti, E., Guizani, M.: Impact of non-linear high-power amplifiers on cooperative relaying systems. IEEE Trans. Commun. **65**(10), 4163–4175 (2017)
17. Kingma, D.P., Ba, J.: Adam: a method for stochastic optimization. arXiv preprint arXiv:1412.6980 (2014)
18. Candreva, E.A., Tarchi, D., Vanelli-Coralli, A., Corazza, G.E.: Robust SC-FDMA subcarrier mapping for non-linear channels. In: 2014 7th Advanced Satellite Multimedia Systems Conference and the 13th Signal Processing for Space Communications Workshop (ASMS/SPSC), pp. 360–365. IEEE (2014)
19. Saleh, A.A.: Frequency-independent and frequency-dependent nonlinear models of TWT amplifiers. IEEE Trans. Commun. **29**(11), 1715–1720 (1981)